Supporting information

Metal-Organic Framework Template Derived Hierarchical Mo-doped LDHs@MOF-Se Core-Shell Array Electrode for Supercapacitors

Yulu Zhu [a], Wei Du [a], Qilong Zhang *[a], Hui Yang [a, b], Quan Zong [a], Qianqian Wang [a], Zheng Zhou[a], Jianhui Zhan[a],

a School of Materials Science and Engineering, State Key Lab Silicon Mat, Zhejiang University, Hangzhou 310027, PR China

b Zhejiang California International NanoSystems Institute, Zhejiang University, Hangzhou 310058, China.

* Corresponding author. E-mail address: mse237@zju.edu.cn

1.Experimental Section

1.1. Synthesis of MOF NA. For the synthesis of MOF array electrode, 0.3 mmol of Zn $(NO_3)_2 \cdot 6H_2O$, 0.6 mmol of Co $(NO_3)_2 \cdot 6H_2O$ were dissolved in 20 mL of deionized water under stirring to get solution A, and 7.5 mmol of 2-methylimidazole (2-MIM) was dispersed in 20 mL deionized water to get solution B. Subsequently the two kinds of solution were quickly mixed, a slice of treated carbon cloth (CC) was immerged in the mixture and then put to a Teflon-lined autoclave. Soon afterwards, it was heated up and held at 70 °C for 240 min in an oven. Behind cooling down the CC with active materials were cleaned with deionized water and ethanol, finally dried at 60 °C to get the purple MOF/CC product.

1.2. Synthesis of MOF-Se NA. 600mg Se powders and the as-prepared MOF /CC were put at upstream and downstream of the tubular furnace, respectively. Then, the furnace was heated to 450 ℃ in 90 min and maintained for 120 min under argon atmosphere and then cooled down, the product was marked as MOF-Se /CC

1.3. Electrodeposition process of Mo-doped LDHs. Electrodeposition process were executed in a conventional three-electrode electrochemical mode with MOF-Se /CC as the working electrode, a Pt plate and a Ag/AgCl electrode was taken for the counter electrode and the reference electrode, 100 ml distilled water containing 0.005 mol $Ni(NO_3)_2 \cdot 6H_2O$, 0.005 mol $Co(NO_3)_2 \cdot 6H_2O$ and 0.0025 mol $(NH_4)_6Mo_7O_{24} \cdot 4H_2O$ served as the electrodeposition solution. The process was executed at a constant potential of -1.0 V for 600 s, and the mass of active materials was about 5mg cm^{-2}. And

the LDHs@MOF-Se electrode was synthesized as the same process except no $(NH_4)_6Mo_7O_{24}{\cdot}4H_2O$ added.

1.4. Electrochemical tests. The tests of the as-fabricated electrodes were tested in a routine three-electrode mode, where the as-tested electrodes were employed as working electrode and the sample contacted the electrolyte area was 1 cm^2, and platinum plate (1*1 cm^2) and Hg/HgO electrode used as counter electrode and reference electrode, respectively, and 3 M KOH aqueous solution for the electrolyte. The area specific capacity (Q) (C cm^{-2}) can be counted based on the GCD results using the formula (1):

$$Q = I\Delta t/s \tag{1}$$

and I is the charging current (mA), Δt refers to the discharging period (s) and s refers to the area of tested electrode (cm^2).

Electrochemical impedance spectroscopy (EIS) was obtained in the frequency between 0.01 to 10^5 Hz at open-circuit voltage.

1.5. Assembly of the Asymmetric Supercapacitor (ASC). ASC was fabricated using the Mo-doped LDHs@MOF-Se electrode for the positive electrode and the active carbon (AC) electrode as the negative electrode and name as Mo-doped LDHs@MOF-Se//AC and tested in a two-electrode mode.

The value of energy density (E), power density (P) are determined in accordance with the formula below:

$$E = \frac{Q\Delta V^2}{2 \times 3.6} \tag{2}$$

$$P = \frac{3600E}{\Delta t} \tag{3}$$

in which Q represents the specific capacitance (F g^{-1}), ΔV refers to the voltage window (V), and Δt refers to discharging period (s).

2.Material characterization. The X-ray di□raction (XRD) patterns were obtained by X-ray di□reaction (XRD, X' Pert 168 PRO, PANalytical, Netherlands) using Cu Kα radiation. X-ray photoelectron spectroscopy (XPS) technique (ESCALAB 250 XI) was conducted with an Al Kα radiation (1486.6 eV). Field emission scanning electron microscopic (SEM) images were observed by S-8010(Hitachi Ltd., Japan). TEM images and high-resolution transmission electron microscopy (HRTEM) images were taken on with TEM (Tecnai G2 F20, FEI Co., Netherlands) equipment.

Energy dispersive X-ray spectra (EDS) was tested through HRTEM.

3. Supplementary Figures

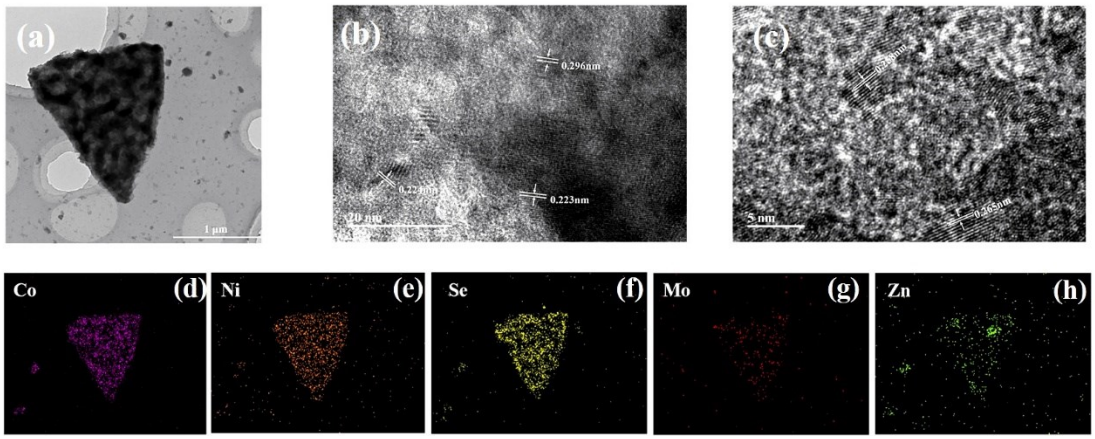

Fig. S1 (a) TEM images of Mo-doped LDHs@MOF-Se; (b)HRTEM of Mo-doped LDHs shell; (c)HRTEM of MOF-Se core;(d-h) the elemental mapping images of Mo-doped LDHs@MOF-Se.

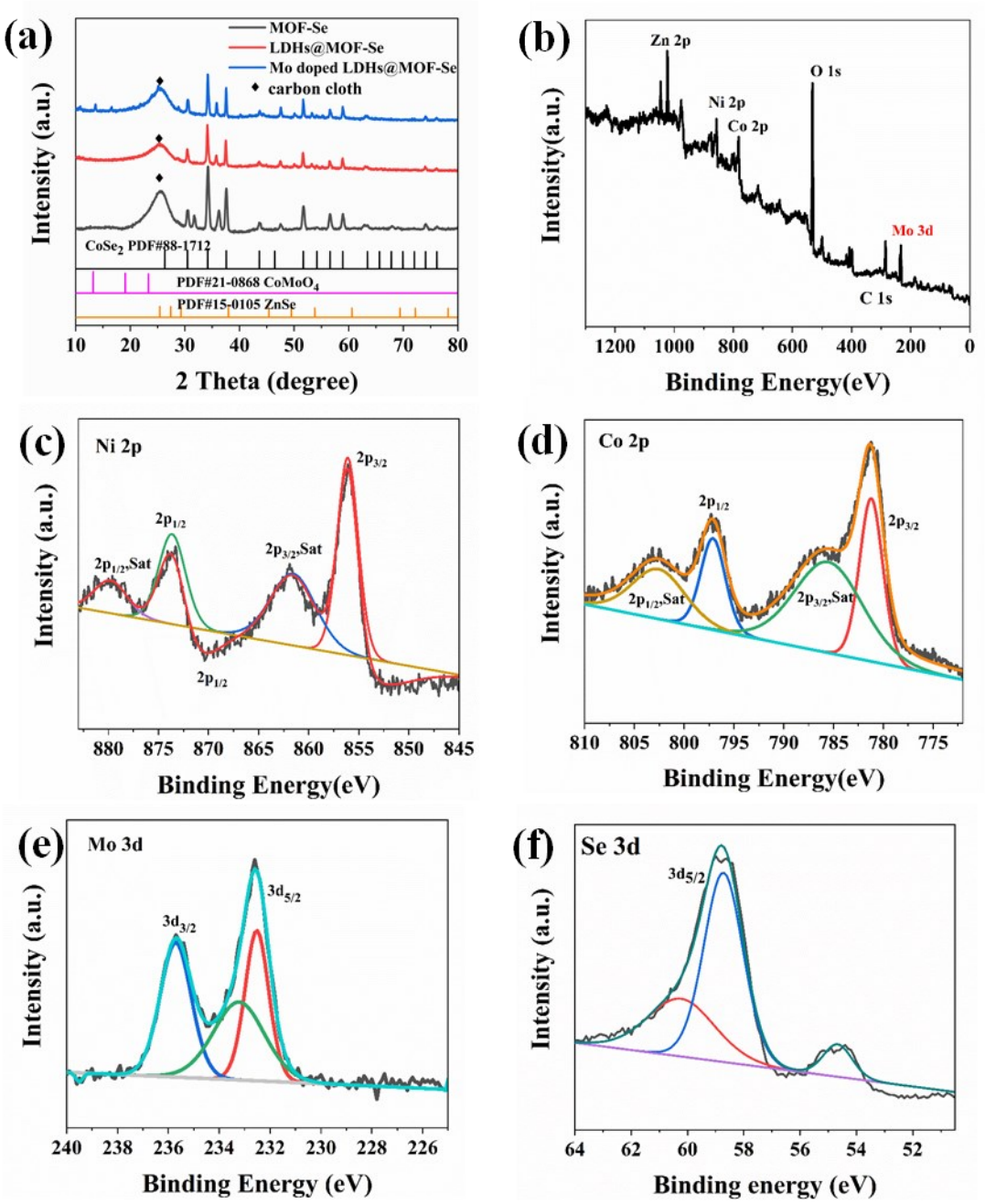

Fig. S2 (a) XRD spectra of the fabricated samples; (b) overall XPS spectrum and high-resolution XPS spectra of (c)Ni 2p, (d)Co 2p, (e)Mo 3d and (f) Se 3d

The characteristic XRD diagram of the products are depicted in Fig. S2. The XRD patterns of MOF-Se is well-matched to $CoSe_2$ and ZnSe, and the di□raction angles of MOF-Se situated at 2θ=34.19, 37.57, 43.65, 51.70, 56.59, 58.93 and 69.40° correspond to (210), (211), (220), (311), (023), (321) and (202) planes of $CoSe_2$ (JCPDS #88-1712) [1]and planes of ZnSe (JCPDS #15-0105)[2], respectively. After the electrodeposition treatment, these peaks assigned to MOF-Se were still

visible and the newly appeared diffraction peaks of Mo-doped LDHs@MOF-Se can be assigned to the $CoMoO_4$ phase (JCPDS #21-0868)[3], indicating the successful doping of Mo and the original MOF-Se structure well maintained. There are no obvious peaks attributed to the LDHs phase on account of the poor crystallization of the LDHs.

XPS was further executed to probe the electronic states and chemical constitution of the products. As displayed as Fig. S2b, the full spectrum of the as-fabricated Mo-doped LDHs@MOF-Se uncovers the existence of Ni, Co, Zn, Mo, Se, O and C element. With regard to high resolution XPS spectra, the Ni $2p_{1/2}$ and Ni $2p_{3/2}$ (Fig. S2c) can be noticed at 871.5 and 856.1 eV. Three shake-up satellite peaks of Ni 2p situated at 873.6, 879.8 and 861.5 eV are also observed[4]. The main peaks at 781.2 eV and 797.1 eV of Co 2p spectrum are observed, which are attributed to the Co $2p_{3/2}$ and Co $2p_{1/2}$ spin orbital coupling[5], which verifies the presence of Co^{2+} and Co^{3+} in this material. Besides, the Mo $3d_{3/2}$ and Mo $3d_{5/2}$ at 235.7 and 232.5 eV manifest the distinctive Mo^{6+}-doping in Mo-doped LDHs@MOF-Se sample. Besides, the fitting peaks of Se_{3d} at 57.0-62.0 eV, assigned to SeO_x.

The electrode kinetics are uncovered by EIS. To be specific, the diameter of the semicircle in the high-frequency range refers to the charge-transfer resistance, and the line slope in the low-frequency range refers to the diffusion resistance (R_w) and the intersections on the X-axis at high frequency refer to the electrolyte resistance (R_S), composed of the interface resistance, the internal resistance, and the ionic resistance of the electrolyte.

To uncover the electrochemical kinetics and reaction kinetics of electrode materials, CV tests were carried out. Fig. S3a displays the CVs of the Mo-doped LDHs@MOF-Se electrode at various scan rates of 1 to 5 mV s^{-1} and the curves are similar in incremental scanning rate. The total capacity of an electrode can be divided into two parts, including the diffusion controlled and the capacity controlled which does not rely on the current density or the scan rate. The degree of capacitive impact quantitatively follows the below equation:

$$i = av^b$$

where i represents the peak current, v represents the scan rate, and a, b are constants. The value of b varies between 0.5 and 1.0, which can be obtained from the slope of the log(i) versus log (v) plot.

With regard to a di□usion-dominated course the b value is close to 0.5, whereas when a surface capacitive contribution plays a leading role, the b value approximates 1.0. The obtained b value for Mo-doped LDHs@MOF-Se and LDHs@MOF-Se electrodes is 0.683, 0.742, respectively. When the potential is fixed, the corresponding current response i can be divided into capacitance-dominated reactions ($k_1 v$) and di□usion-dominated ($k_2 v^{1/2}$), following the equation:

$$i(V) = k_1 v + k_2 v^{1/2}$$

Where $i(V)$, v, k_1 and k_2 represents the current, scan rate and constants. That formula can be deformed into:

$$i(V)/v^{1/2} = k_1 v^{1/2} + k_2$$

By plotting $i(V)/v^{1/2}$ vs. $v^{1/2}$ varies potentials, the values of k_1 (slope) and k_2 (intercept) can be obtained by fitting the test data. The portion of capacitance-controlled capacity and diffusion-dominated course can be separated when the values of k_1 and k_2 are gotten. Fig. S3c shows comparison of the capacitive contribution of Mo-doped LDHs@MOF-Se is 39.8%, 52.2%, 61.2%, 68.2% and 70.2% at the scan rate of 1, 2, 3, 4 and 5mV s^{-1}, respectively. The parallel table of electrodes at various scan rates is depicted in Fig.S3d. It can be observed that the kinetics of Mo-doped LDHs@MOF-Se electrode is dominated by capacitive process.

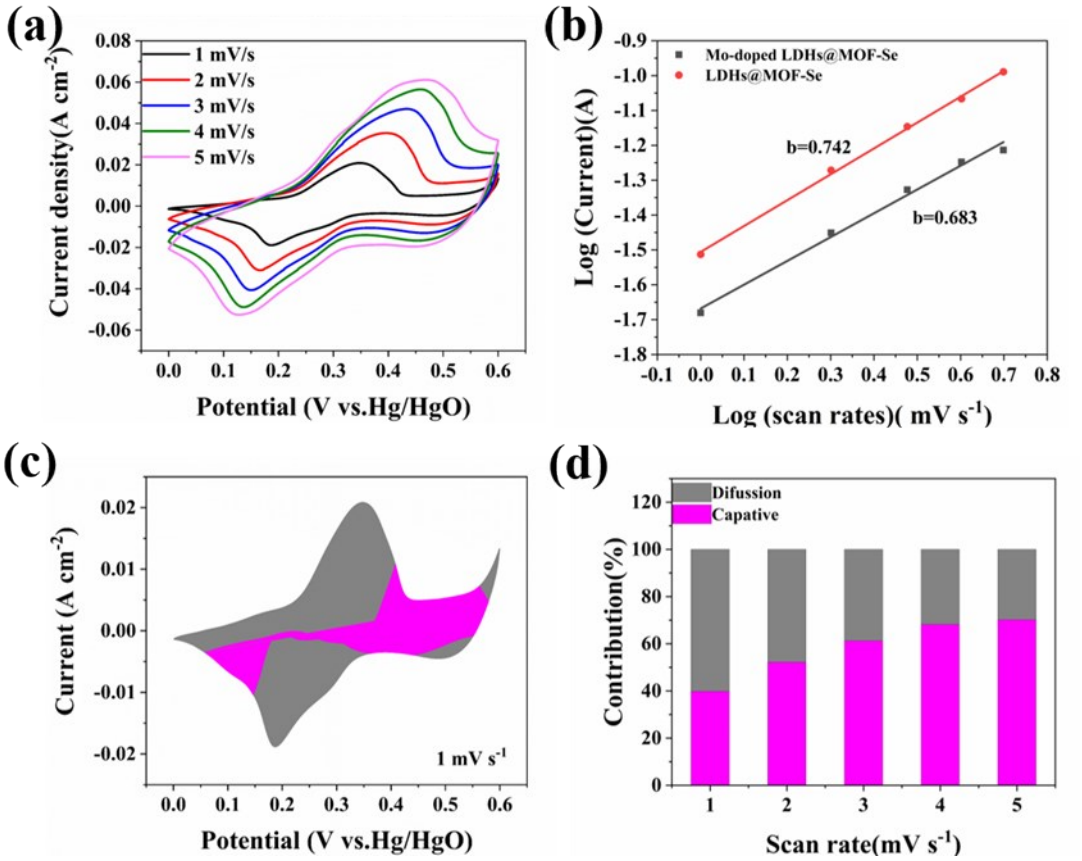

Fig. S3. (a) CV plots of the Mo-doped LDHs@MOF-Se electrode; (b) logarithmic relation between anodic peak current and sweep rate; (c) capacitive contribution and diffusion contribution of Mo-doped LDHs@MOF-Se; (d) comparison of capacitive contribution at different scan rates.

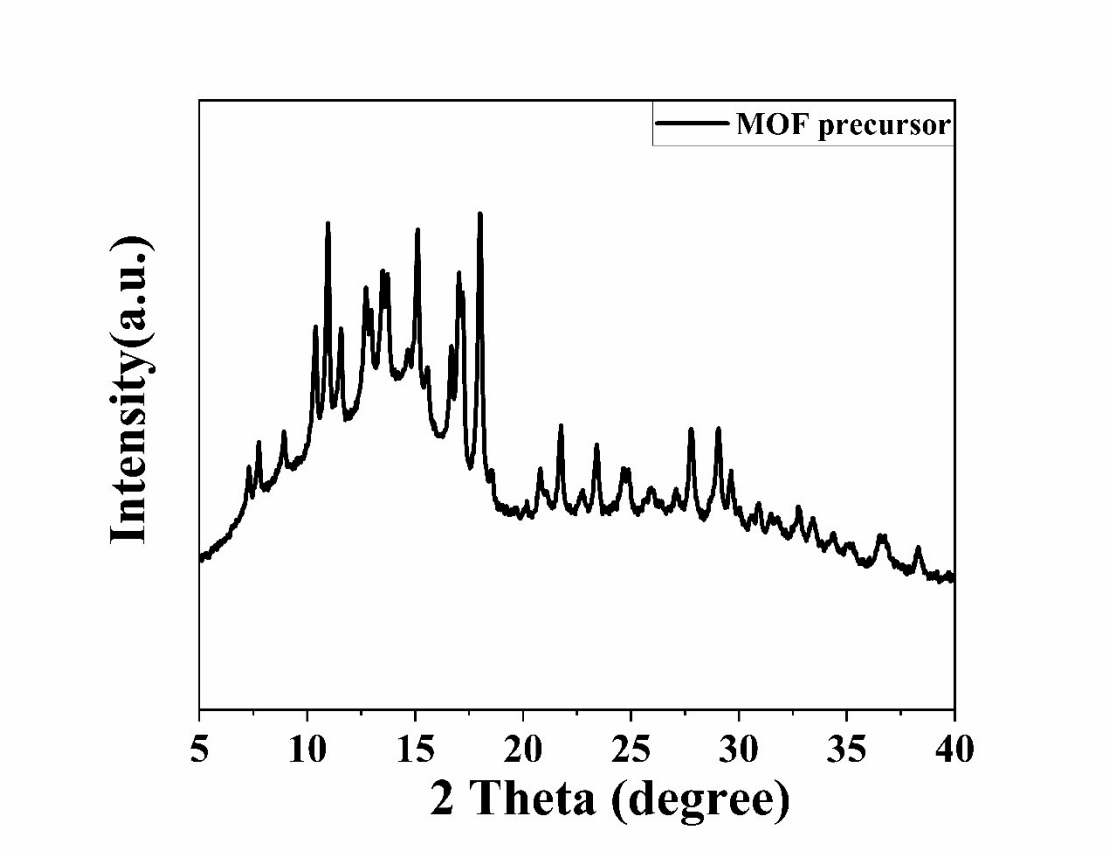

Fig. S4. XRD spectra of the fabricated MOF precursor.

The Brunauer–Emmet–Teller (BET) surface areas of the MOF. MOF-Se and Mo-doped LDHs@MOF-Se are calculated to be 55.436 ,79.017 and 57.331 $m^2 g^{-1}$.

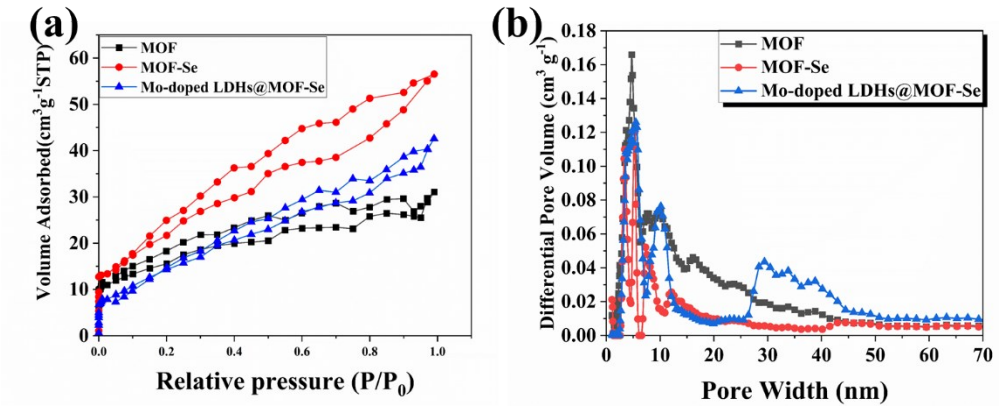

Fig. S5. (a) Nitrogen adsorption and desorption isotherms plots; (b)Pore size distribution plots.

Table S1. Comparison of Our Electrode Supercapacitor Performance with Pervious Analogous Electrodes

Composites	Morphology	Specific Capacitance	Rate retention	Cycle stability	Energy density (Wh kg^{-1})	Power Density (W kg^{-1})	Article
Mo-doped LDHs@MOF-Se	Core-shell	10.32 F cm^{-2} (1 mA cm^{-2})	91.9 %	81.4 % (3000 cycles)	41.3	750.0	**This work**
$ZnCo_2O_4$@$Ni(OH)_2$	Core-shell	3.06 F cm^{-2} (1 mA cm^{-2})	55.3%	50.1%, (5000 cycles)	40.0	8020	[6]
NiCo-LDH/Co_9S_8	Core-shell	2.14 F cm^{-2} (1 A g^{-1})	72.4%	92.6% (5000 cycles)	38.0	800	[7]
NiCo-LDH derived from MOF	nanosheet	2.22 F cm^{-2}	89.2%	95.0% (2000 cycles)	59.2	850	[8]
(Ni,Co)Se_2/NiCo-LDH	Cactus-Like	0.816 F cm^{-2} (1 mA cm^{-2})	71 %	89.5% (3000 cycles)	39	1650	[9]

ASC assembled by Mo-doped LDHs@MOF-Se and AC displays a high energy density of 41.3 Wh kg^{-1} with a power density of 750.0 W kg^{-1} and holds 29.1 Wh k_g^{-1} with a power density 3500.0 W kg^{-1} surpass the performances of the similar device reported such as $ZnCoO_4$@$Ni(OH)_2$//AC(40 Wh kg^{-1} with 802.7 W kg^{-1}), Ni-doped cobalt-cobalt nitride//AC(29.08 Wh kg^{-1} at 980 W kg^{-1}), (Ni,Co)Se_2/NiCo-LDH (39 Wh kg^{-1} with 1650W kg^{-1}), NiSe@$Co_2(CO_3)(OH)_2$//AC(35.5 Wh kg^{-1} with 1280 W kg^{-1}), Ni_2Se_3(32.8 Wh kg^{-1} with 677.0 W kg^{-1}).

(1) Ge, P.; Hou, H. S.; Li, S. J.; Huang, L. P.; Ji, X. B. *ACS Appl. Mater. Interfaces* **2018**, *10*, 14716.

(2) Achimovicova, M.; Balaz, P.; Ohtani, T.; Kostova, N.; Tyuliev, G.; Feldhoff, A.; Sepelak, V. *Solid State Ion.* **2011**, *192*, 632.

(3) Wang, X. H.; Rong, F.; Huang, F. F.; He, P.; Yang, Y.; Tang, J. P.; Que, R. H. *J. Alloy. Compd.* **2019**, *789*, 684.

(4) Cebada, S.; Soto, E.; Mota, N.; Fierro, J. L. G.; Navarro, R. M. *Int. J. Hydrog. Energy* **2020**, *45*,

20536.

(5) Wang, L. L.; Guo, X.; Chen, Y. Y.; Ai, S. S.; Ding, H. M. *Appl. Surf. Sci.* **2019**, *467*, 954.

(6) Han, X.; Yang, Y. J.; Zhou, J. J.; Ma, Q. X.; Tao, K.; Han, L. *Chem.-Eur. J.* **2018**, *24*, 18106.

(7) Yang, Q. J.; Liu, Y.; Xiao, L. S.; Yan, M.; Bai, H. Y.; Zhu, F. F.; Lei, Y.; Shi, W. D. *Chem. Eng. J.* **2018**, *354*, 716.

(8) Wang, T.; Zhang, S. L.; Yan, X. B.; Lyu, M. Q.; Wang, L. Z.; Bell, J.; Wang, H. X. *ACS Appl. Mater. Interfaces* **2017**, *9*, 15510.

(9) Li, X.; Wu, H. J.; Guan, C.; Elshahawy, A. M.; Dong, Y. T.; Pennycook, S. J.; Wang, J. *Small* **2019**, *15*, 10.